Tropolysin, a New Oligopeptidase from African Trypanosomes[†,‡]

Rory E. Morty,*[,§] István Vadász,[§,||] Patrick Bulau,[§] Vincent Dive,[⊥] Vitor Oliveira,[#] Werner Seeger,[§] and Luiz Juliano[#]

Department of Internal Medicine, University Hospital Giessen, Aulweg 123, D-35392 Giessen, Germany, Commissariat à l'Energie Atomique, Direction des Sciences du Vivant, CE-Saclay 91191, Gif-sur-Yvette Cedex, France, and Departamento de Biofísica, Escola Paulista de Medicina, Universidade Federal de São Paulo, Rua Três de Maio 100, São Paulo 04044-020, Brazil

Received June 1, 2005; Revised Manuscript Received August 22, 2005

ABSTRACT: Oligopeptidases are emerging as important pathogenic factors and therapeutic targets in trypanosome infections. We describe here the purification, cloning, and biochemical analysis of a new oligopeptidase from two pathogenic African trypanosomes. This oligopeptidase, which we have called tropolysin (encoded by the *trn* gene), represents an evolutionarily distant member of the M3A subfamily of metallopeptidases, ancestral to thimet oligopeptidase, neurolysin, and saccharolysin. The *trn* gene was present as a single copy per haploid genome, was expressed in both the mammalian and insect stages of the parasite life cycle, and encoded an 84 kDa protein. Both purified and hyperexpressed tropolysin hydrolyzed bradykinin-derived fluorogenic peptide substrates at restricted sites, with an alkaline pH optimum, and were activated by dithiothreitol and reduced glutathione and by divalent metal cations, in the order $Zn^{2+} > Co^{2+} > Mn^{2+}$. Under oxidizing conditions, tropolysin reversibly formed inactive multimers. Tropolysin exhibited a preference for acidic amino acid side chains in P_4, hydrophobic side chains in P_3, and hydrophobic or large uncharged side chains in P_1, P_1', and P_3', while the S_2' site was unselective. Highly charged residues were not tolerated in P_1'. Tropolysin was responsible for the bulk of the kinin-degrading activity in trypanosome lysates, potently ($k_{cat} \approx 119\ s^{-1}$) inactivated the vasoactive kinins bradykinin and kallidin, and generated angiotensin(1−7) from angiotensin I. This hydrolysis both abolished the capacity of bradykinin to stimulate the bradykinin B_2 receptor and abrogated bradykinin prohypotensive properties in vivo, raising the possibility that tropolysin may play a role in the dysregulated kinin metabolism observed in the plasma of trypanosome-infected hosts.

African trypanosomes of the genus *Trypanosoma* are pathogenic protozoan parasites that cause fatal disease in humans and animals in sub-Saharan Africa. *Trypanosoma brucei rhodesiense* and *Trypanosoma brucei gambiense* cause acute and chronic human African sleeping sickness, respectively, placing 60 million people at risk with 50000 deaths reported per year, while the related trypanosome *Trypanosoma brucei brucei* causes bovine African trypanosomiasis or *nagana* (*1*). Africa is currently experiencing a massive resurgence in the incidence of both human and bovine forms of this disease as well as in drug resistance by trypanosomes (*1*); thus there is a pressing need for the identification of novel virulence factors, drug targets, and vaccines to improve our understanding, treatment, and prevention of African trypanosomiasis.

The peptidases of parasitic protozoans are emerging as important virulence factors, drug targets, and vaccine candidates in trypanosome infections and include a cell surface metallopeptidase, lysosomal cysteine peptidases, the proteasome, and cytosolic serine oligopeptidases (*2*). Trypanosome oligopeptidases in particular have demonstrated exciting potential both as virulence factors and as therapeutic targets. To date, only one group of oligopeptidases has received attention: the prolyl oligopeptidase (S9A) subfamily of serine peptidases, represented by prolyl oligopeptidase (EC 3.4.21.26; POP)[1] and oligopeptidase B (EC 3.4.21.83; OpdB). Both POP (*3*) and OpdB (*4*) have been described from the South

[†] Supported by the Alexander von Humboldt Foundation, the Deutsche Forschungsgemeinschaft SFB 547, the Commissariat à l'Energie Atomique, the Fundação de Amparo à Pesquisa do Estado de São Paulo, and the Conselho Nacional de Desenvolvimento Científico e Tecnológico.

[‡] The GenBank/EBI database accession numbers for the *trn* genes are AY623661 (*T. brucei brucei*) and AY623662 (*T. brucei rhodesiense*).

* To whom correspondence should be addressed. Tel: +49 641 994 2303. Fax: +49 641 994 2308. E-mail: rory.morty@innere.med.uni-giessen.de.

[§] University Hospital Giessen.

[||] Present address: Division of Pulmonary and Critical Care Medicine, Feinberg School of Medicine, Northwestern University, 240 East Huron Ave., McGaw 2300, Chicago, IL 60611.

[⊥] Commissariat à l'Energie Atomique.

[#] Universidade Federal de São Paulo.

[1] Abbreviations: Abz, *o*-aminobenzoyl; AMT, acetate−Mes−Tris; ANF, atrial natriuretic factor; AngI, angiotensin I; BK, bradykinin; Cbz, N^{α}-carbobenzyloxy; DCP, dipeptidyl carboxypeptidase; Dnp, 2,4-dinitrophenyl; E-64, L-*trans*-epoxysuccinylleucylamido(4-guanidino)-butane; EST, expressed sequence tag; GAPDH, glyceraldehyde-phosphate dehydrogenase; Mca, (7-methoxycoumarin-4-yl)acetyl; Mes, 4-morpholineethanesulfonic acid; MIP, mitochondrial intermediate peptidase; Nle, 2-aminohexanoic acid; OpdB, oligopeptidase B; ORF, open reading frame; POP, prolyl oligopeptidase; SSC, sodium chloride/sodium citrate; TOP, thimet oligopeptidase; TPP, three-phase partitioning; Tricine, *N*-[2-hydroxy-1,1-bis(hydroxymethyl)ethyl]glycine.

10.1021/bi051035k CCC: $30.25
Published on Web 10/14/2005

American trypanosome, *Trypanosoma cruzi*, the etiological agent of Chagas' disease, in which POP has been designated as a chemotherapeutic target (*5*), and both POP and OpdB have been validated as virulence factors (*4*, *6*). Oligopeptidase B (but not POP) has been described from *Trypanosoma brucei* (*7*), *Trypanosoma congolense* (*8*), and *Trypanosoma evansi* (*9*). Drugs used to treat African trypanosomiasis inhibit OpdB (*10*), and specific OpdB inhibitors exhibit antitrypanosome activity and improve outcome in a mouse model of *T. brucei* infection (*11*), implicating OpdB as a therapeutic target. Oligopeptidase B has also been validated as a virulence factor in African trypanosomes, since it is released into the host circulation by dead and dying parasites (*9*), where it retains catalytic activity and degrades regulatory peptides such as atrial natriuretic factor (ANF) (*9*), thereby reducing circulating levels of these peptides, with serious consequences for the metabolic homeostasis of the host. Other studies have indicated that, in addition to OpdB, a trypanosome-derived cation-sensitive, thiol-dependent peptidase with kinin-degrading (kininase) activity was active in the plasma of infected hosts (*12*), although this peptidase was not identified. Thus, we set out to identify and characterize novel oligopeptidases from African trypanosomes, specifically those with kininase activity.

In the present study we describe the purification, cloning, genetic analysis, and kinetic properties of a new oligopeptidase from two pathogenic African trypanosomes. This oligopeptidase, which we have called tropolysin [*tr*ypanosome *o*ligo*p*eptidase (metallopeptidase), encoded by the *trn* gene], represents a new member of the M3A subfamily of metallopeptidases and is most closely related to the eukaryotic thimet oligopeptidase/neurolysin cluster within this group of enzymes. This is the first report of any member of the M3 family of metallopeptidases from any protozoan organism. Tropolysin exhibits a unique substrate specificity within the M3A subfamily and appears to be the primary kininase activity in trypanosome extracts. This may have significant implications for the pathogenesis of African trypanosomiasis. Since tropolysin is also one of the most evolutionarily divergent members of the M3A subfamily of metallopeptidases, this study provides new data on the enzymology of this interesting family of peptidases and expands our knowledge of the peptidolytic capacity of African trypanosomes, which up until now has been limited to four peptidases.

EXPERIMENTAL PROCEDURES

Parasites. T. brucei brucei ILTat 1.1 was originally isolated from naturally infected bovine blood in Utembo, Kenya, while *T. brucei rhodesiense* IL3953 was originally isolated from infected human blood in Nairobi, Kenya (*9*). Bloodstream-form trypanosomes were either maintained in culture or passaged in rats, and procyclic *T. brucei brucei* ILTat 1.1 (tsetse fly midgut stage) were cultured and isolated as described previously (*9*). Experimental animal protocols were approved by local and national authorities.

Enzyme Assays. Tropolysin activity was measured against a modified bradykinin (BK) substrate (7-methoxycoumarin-4-yl)acetyl-Arg-Pro-Pro-Gly-Phe-Ser-Ala-Phe-Lys(2,4-dinitrophenyl) [Mca-(Ala^7,Lys(Dnp)^9)-BK; Bachem]. Activity was determined in 50 mM Tris-HCl, 100 mM NaCl, and 0.05% (v/v) Brij 35, pH 8, containing 0.1 mM DTT and 10 mM $CaCl_2$ in an Hitachi F-2000 spectrofluorometer (λ_{ex} = 320 nm, and λ_{em} = 405 nm). Active enzyme concentration ($[E]_0$) was determined by active site titration against Cbz-$_{(L,D)}$Pheψ(PO_2CH_2)$_{(L,D)}$Ala-Arg-Tyr (*13*) as described previously (*14*).

Kininase Activity in Parasite Lysates. Purified parasites were resuspended in 50 mM Tris-HCl and 100 mM NaCl, pH 7.4, containing 0.1 mM DTT and 10 mM $CaCl_2$. Parasite extracts were prepared by one freeze−thaw cycle, and addition of Triton X-100 to 0.1% (v/v), and clarified by centrifugation (15000*g*, 30 min, 4 °C) (*7*). Hydrolytic activity of parasite extracts was assayed against Mca-(Ala^7,Lys-(Dnp)^9)-BK as described above, either alone or in the presence of 1 mM 3,4-dichloroisocoumarin (DCI), 10 μM L-*trans*-epoxysuccinylleucylamido(4-guanidino)butane (E-64), 1 mM 1,10-phenanthroline, or 10 μM pepstatin A, to detect serine, cysteine, metallopeptidase, and aspartic peptidase activity, respectively. All assays were conducted at pH 7.4 to approximate physiological pH.

Purification of Tropolysin and Cloning, Sequencing, Genomic Analysis, in Vivo Expression, and Site-Directed Mutagenesis of the Tropolysin-Encoding Gene. Methodological details describing the purification of tropolysin from *T. brucei brucei* ILTat 1.1 lysates and the cloning, sequencing, genomic analysis, in vivo expression, and site-directed mutagenesis of the *trn* gene are described in the Supporting Information.

Enzymatic Characterization of Tropolysin. The pH profile for native tropolysin purified from *T. brucei brucei* was determined by preincubating tropolysin (5 nM, active concentration, 37 °C, 5 min) in constant ionic strength acetate−Mes−Tris (AMT) buffers (50 mM acetic acid, 50 mM Mes, 100 mM Tris-HCl, pH 4−11, with 0.1 mM DTT and 10 mM $CaCl_2$), prior to the addition of Mca-(Ala^7,Lys-(Dnp)^9)-BK substrate. The k_{cat} and K_m were determined as described for substrate specificity; see below.

The metal ion dependence of native tropolysin purified from *T. brucei brucei* was investigated by buffer-exchanging tropolysin into $CaCl_2$-free buffer (5 mM Tris-HCl, 100 mM NaCl, pH 8) on a PD-10 column. The solution was made to 10 mM EDTA, and stored at 4 °C for 24 h (*15*). Metal-depleted tropolysin (apotropolysin) was buffer-exchanged back into EDTA-free buffer, and preincubated (5 min, 37 °C) in the presence of various metal chlorides, prior to the addition of Mca-(Ala^7,Lys(Dnp)^9)-BK substrate, from which the specific activity was determined.

The thiol dependence of native tropolysin purified from *T. brucei brucei* was investigated by buffer exchanging tropolysin into DTT-free buffer (5 mM Tris-HCl, 100 mM NaCl, 10 mM $CaCl_2$, pH 8) on a PD-10 column. Tropolysin was incubated for 24 h at 4 °C in DTT-free buffer to promote inactivation. Tropolysin was preincubated (5 min, 37 °C) in the presence of DTT (0−2 mM) or reduced glutathione (GSH, 0−8 mM) prior to the addition of Mca-(Ala^7,Lys-(Dnp)^9)-BK substrate, from which the specific activity was determined. To investigate whether tropolysin formed multimers under nonreducing conditions, tropolysin was incubated (24 h, 4 °C) in 50 mM Tris-HCl, 100 mM NaCl, and 10 mM $CaCl_2$, pH 8, in either the presence or absence of 100 μM DTT. Samples were resolved by passage over a Sephacryl S-200 HR column (1250 × 15 mm, 0.24 mL·min^{-1})

equilibrated in 50 mM Tris-HCl, 100 mM NaCl, and 10 mM $CaCl_2$, pH 8, in the presence or absence of 100 μM DTT. In both instances, column fractions were reduced with 100 μM DTT prior to assaying hydrolytic activity against Mca-(Ala^7,-Lys(Dnp)^9)-BK.

Substrate specificity of native tropolysin purified from *T. brucei brucei* and recombinant tropolysin from both parasites was explored using a series of intramolecularly quenched fluorogenic peptide substrates based on the core BK sequence of the general formula *o*-aminobenzoyl (Abz)-Gly-Phe-Ser-Pro-Phe-Arg-Gln-2,4-ethylenediamine (EDDnp), synthesized as described previously (*14*). Substrate specificity was determined by preincubation of tropolysin (1−5 nM, active concentration, 37 °C, 1 min) in 50 mM Tris-HCl, 100 mM NaCl, and 0.05% (v/v) Brij 35, pH 8, containing 0.1 mM DTT and 10 mM $CaCl_2$, prior to the addition of substrate. The K_m, V_{max}, and k_{cat} were determined exactly as described previously (*7*). In some instances, peptides were cleaved at two separate sites in the same reaction (F↓S and P↓F), in which case the V_{max} and, hence, k_{cat} for the two separate reactions were determined simultaneously as described previously (*14*, *16*).

Inhibition of tropolysin by metallopeptidase inhibitors, metal ion chelators, and alkylating agents was determined by preincubation of tropolysin (5 nM, active concentration) in 50 mM Tris-HCl, 100 mM NaCl, and 0.05% (v/v) Brij 35, pH 8, containing 0.1 mM DTT containing the relevant inhibitor, prior to determination of activity against Mca-(Ala^7,Lys(Dnp)^9)-BK. For slow, tight-binding ($[E]_0/K_i > 0.01$) inhibitors, the K_i was calculated as described previously (*17*), although a longer preincubation of tropolysin (for 24 h) either alone or in the presence of inhibitor ($0.5-5[E]_0$) was employed (*13*).

Hydrolysis of regulatory peptides was monitored by high-performance liquid chromatography (HPLC) on a μBondapack C18 column (Waters) and by matrix-assisted laser desorption/ionization time-of-flight (MALDI-TOF) mass spectrometry, on a Voyager-DE STR (Applied Biosystems), using α-cyanohydroxycinnamic acid as matrix, exactly as described previously (*9*).

Bioassay for BK B_2 Receptor Activation. The isolated guinea pig ileum assay was employed to investigate BK B_2 receptor activation by BK and its degradation products after hydrolysis by tropolysin, as described previously (*18*), except that 50 nM atropine was incorporated into Tyrode's solution.

Bioassay for BK Prohypotensive Activity. New Zealand white rabbits (≈3 kg) were anesthetized and catheterized exactly as described previously (*9*). After 20−30 min equilibration, a 2 mL bolus of 50 mM Tris-HCl and 100 mM NaCl, pH 8, containing 0.1 mM DTT and 10 mM $CaCl_2$, was infused over 30 s via a three-way stopcock in the right ear vein catheter (volume control). Subsequently, intact BK (10 nmol·kg^{-1}, in 2 mL) was infused, followed by BK (10 nmol·kg^{-1}, in 2 mL) that had been preincubated with catalytically active recombinant tropolysin at a 1:50 (mol/mol, by activity/mass) tropolysin:BK ratio for 1 h at 37 °C or with a catalytically inactive recombinant tropolysin-(E532Q) at a 1:50 (mol/mol, by mass/mass) ratio for 1 h at 37 °C. Finally, catalytically inactive recombinant tropolysin-(E532Q) [0.2 nmol (by mass)·kg^{-1}, in 2 mL] was applied as a bolus over 30 s. The mean arterial pressure (MAP) was allowed to stabilize (≈20 min) between applications.

Statistics. Intergroup differences were estimated by a statistical analysis of variance (ANOVA). Fisher's protected least significant difference test was employed to compare individual groups. Differences within the same group were evaluated with Student's *t*-test.

RESULTS AND DISCUSSION

Kininase Activity of T. brucei brucei Lysates. The kininase activity of *T. brucei brucei* lysates was evaluated against the BK-derived substrate Mca-(Ala^7,Lys(Dnp)^9)-BK. The Mca-(Ala^7,Lys(Dnp)^9)-BK-hydrolyzing activity was inhibited 70 ± 5% by 1,10-phenanthroline and 25 ± 3% by DCI, implicating both metallopeptidase and serine peptidase activity (data not shown). Multiple BK-degrading metalloendopeptidases have been described from mammals, including meprin, neutral endopeptidase, thimet oligopeptidase, angiotensin I-converting enzyme, neurolysin, and mitochondrial intermediate peptidase (*19*). However, no homologues of any of these enzymes have been described from protozoans. We therefore set out to purify the enzyme(s) responsible for this activity from trypanosome lysates.

Purification of a Mca-(Ala^7,Lys(Dnp)^9)-BK-Degrading Metallopeptidase from T. brucei brucei Lysates. A Mca-(Ala^7,Lys(Dnp)^9)-BK-degrading metallopeptidase, which we have called tropolysin, was purified from *T. brucei brucei* lysates 39-fold in a six-step procedure with a 0.98% yield (Table S1; see Supporting Information). The purified enzyme was 12% active as judged by active site titration and had a molecular mass of ≈85 kDa by reducing Tris−Tricine SDS−PAGE (Figure S1A; see Supporting Information). Three peptides (boxed, in Figure 1A) obtained from an endoproteinase Glu-C digest of the purified protein displayed sequence similarity to various members of the M3A subfamily of metallopeptidases. One of these peptides, FGHAIH, displayed weak similarity to dipeptidyl carboxypeptidase (DCP; EC 3.4.15.5)) from *Caulobacter crescentus* (*E*-value of 518). A second peptide, XSFGHLTGYG, displayed similarity to a putative mitochondrial intermediate peptidase (MIP; EC 3.4.24.59) from *Cryptococcus neoformans* (*E*-value of 147). A third peptide, MLRNFLGR, displayed strong sequence similarity to thimet oligopeptidase (TOP, EC 3.4.24.15) from *Xenopus laevis* (*E*-value of 4.7) and *Homo sapiens* (*E*-value of 286). Thus, we speculated that the peptidase we had isolated was related to TOP. To confirm the identity of the peptidase, and to facilitate production of recombinant protein, we set out to clone the gene encoding tropolysin from *T. brucei brucei*.

Cloning, Genomic Analysis, and in Vivo Expression of the Tropolysin-Encoding Genes from T. brucei brucei and T. brucei rhodesiense. A 307-bp expressed sequence tag (EST; GenBank/EBI accession number T26735) obtained from a *T. brucei rhodesiense* WRATat1.1 EST library has been described (*20*) that displays 60% similarity to the corresponding sequence from porcine TOP. Using this 307-bp fragment as a probe, we screened a *T. brucei brucei* genomic DNA library and obtained the full coding sequence of the *T. brucei brucei* tropolysin gene, which we designated *trn* (*tr*opolysi*n*). The *T. brucei brucei trn* gene contained an open reading frame (ORF) of 2232 bp, encoding a protein of 84 kDa with a predicted p*I* of 5.91. This sequence has been deposited in the GenBank/EBI database under accession

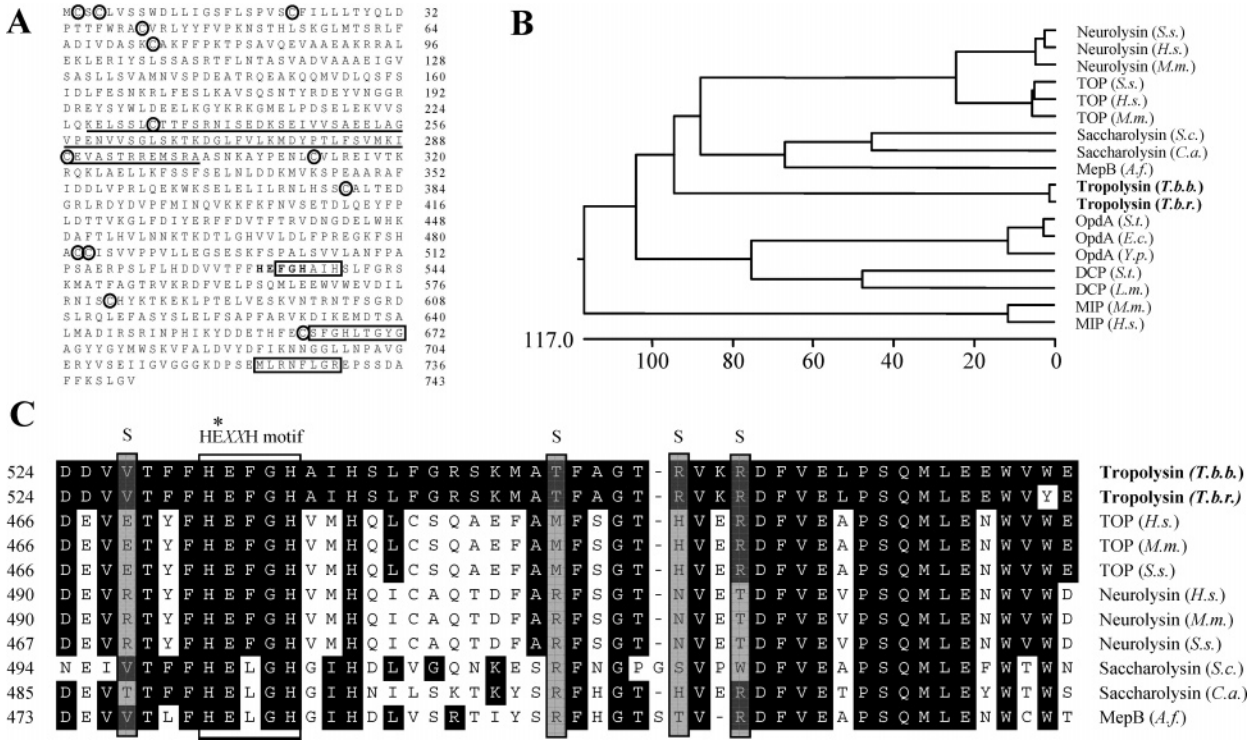

FIGURE 1: Tropolysin from African trypanosomes. (A) Amino acid sequence of tropolysin from *T. brucei brucei*. The sequences of three peptides obtained after endoproteinase Glu-C cleavage of the purified *T. brucei brucei* tropolysin are boxed. Cysteine residues are circled, and the peptide sequence corresponding to the EST sequence used to probe the *T. brucei brucei* library is underlined. The canonical HE*XX*H sequence is in bold type. (B) An unrooted dendrogram comparing full-length amino acid sequences using the CLUSTAL W alignment software of the MEGALIGN program (DNASTAR). The scale at the bottom measures the distance between sequences. Units indicate the number of substitution events. Sequences were obtained from the GenBank/EBI database under the following accession numbers: BAA19060 (*Sus scrofa* neurolysin), CAC27329 (*Homo sapiens* neurolysin), NP_083723 (*Mus musculus* neurolysin), S43250 (*S. scrofa* TOP), AAA82606 (*H. sapiens* TOP), AAG35061 (*M. musculus* TOP), P25375 (*Saccharomyces cerevisiae* saccharolysin), EAK96908 (*Candida albicans* saccharolysin), AAB66656 (*Aspergillus fumigatus* oligopeptidase MepB), AAT46476 (*T. brucei brucei* tropolysin), AAT46477 (*T. brucei rhodesiense* tropolysin), A42298 (*Salmonella enterica* serovar *Typhimurium* OpdA), AAA16155 (*E. coli* OpdA), NP_407415 (*Yersinia pestis* OpdA), A42297 (*S. enterica* serovar *Typhimurium* DCP), NP_047105 (*Leishmania major* DCP), NP_081712 (*M. musculus* MIP), and NP_005923 (*H. sapiens* MIP). (C) Multiple sequence alignment of the amino acid sequences surrounding the catalytic Glu residue (*) and the canonical HE*XX*H motif of 11 members of the M3A subfamily of metallopeptidases. Four substrate-binding residues (S) are indicated. Sequence origins are the same as those used in (B).

number AY623661. Using primers complementary to regions upstream and downstream of the *T. brucei brucei* ORF, the *T. brucei rhodesiense trn* gene was obtained by PCR using genomic DNA from *T. brucei rhodesiense* IL3953 as a template. The *T. brucei rhodesiense trn* gene also contained an ORF of 2232 base pairs, encoding a protein of 84 kDa with a predicted p*I* of 5.73. This sequence has been deposited in the GenBank/EBI database under accession number AY623662. Catalytically active recombinant tropolysins from both parasites were expressed in *Escherichia coli* with an average yield of 8 mg/L of culture.

The tropolysins that we describe here display 97.6% identity to one another at the protein sequence level. Tropolysins display highest (28−29%) sequence identity to mammalian TOPs (Figure 1B), the type peptidase for the M3A subfamily of metallopeptidases. Slightly weaker (27−28%) identity was exhibited with mammalian neurolysin, while even weaker (21−22%) identity was exhibited with bacterial oligopeptidase A. The primary sequence of tropolysin contains the canonical HE*XX*H motif (Figure 1A) that contains the catalytic Glu residue, flanked by two histidine residues that ligate the catalytic zinc atom (*21*, *22*). The tropolysin sequences also contain a third zinc ligand (Glu^{560}) that is conserved in all TOPs (*22*). Additional key residues place the tropolysin closer to the TOP group rather than the neurolysin group. For example, Ala^{607} has been identified as an important determinant of substrate specificity in TOP (*23*) and is conserved among TOPs but is converted to a Gly in neurolysin. This Ala residue is also conserved in tropolysin (Ala^{673}). In addition to sequence differences, tropolysin possesses a 55 amino acid N-terminal extension that is absent in all other members of the M3A subfamily of metallopeptidases. Tropolysin diverges from most other eukaryotic members of the M3A subfamily before the TOP/neurolysin groups diverge from the fungal members of the M3A subfamily, represented by the saccharolysins and oligopeptidase MepB (Figure 1B). Thus, tropolysin is ancestral to TOP, neurolysin, and saccharolysin and represents a novel enzyme.

Trypanosoma genomic DNA digested with restriction endonucleases that do not cut within the *trn* ORF (*Pst*I and *Hin*dIII) yielded single bands on a Southern blot when probed with the full-length *trn* gene. In contrast, endonucleases that cut once within the *trn* ORF (*Drd*I and *Bsa*I) generated two bands (Figure S1B). Thus, the *trn* gene was present as a single copy per haploid *Trypanosoma* genome. Messenger RNA for the *trn* gene was detected in both the bloodstream trypomastigote and the procyclic insect forms of *T. brucei brucei*. Furthermore, messenger RNA was detected in bloodstream-derived and in cultured trypomastigote forms

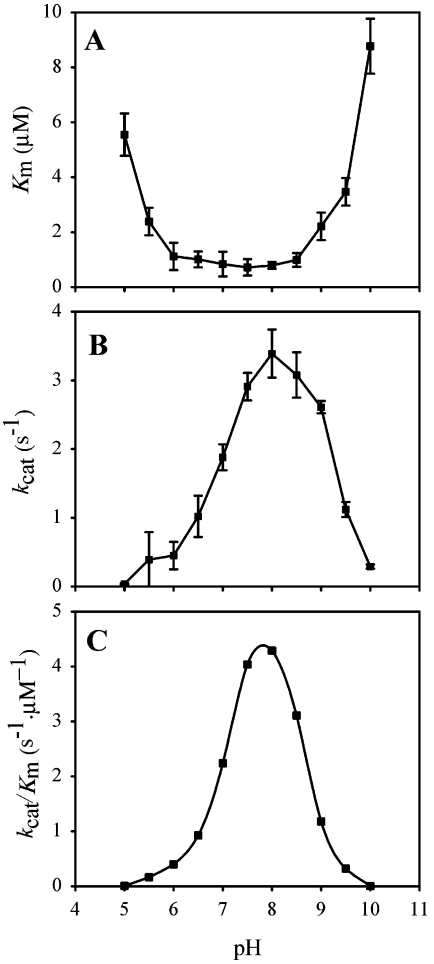

FIGURE 2: pH profile of tropolysin. Kinetic parameters K_m (A) and k_{cat} (B), and thus k_{cat}/K_m (C), were determined for activity of native tropolysin purified from *T. brucei brucei* against Mca-(Ala[7],Lys-(Dnp)[9])-BK in constant ionic strength AMT buffers over the pH range 5−10. Data represent the mean K_m or k_{cat} ± SD ($n = 3$).

of *T. brucei rhodesiense* (Figure S1C) without quantitative differences between the expression levels. These data indicate that the *trn* gene is expressed in mammalian and insect stages of the African trypanosome life cycle.

Kinetic Analysis of Tropolysin. Tropolysin hydrolyzed Mca-(Ala[7],Lys(Dnp)[9])-BK with a K_m of 0.9 μM and a k_{cat} of 4.1 s^{-1} and exhibited an alkaline pH optimum (Figure 2). The K_m was relatively unaffected by pH over the range 6−9 (Figure 2A). In contrast, pH exerted a dramatic effect on the k_{cat} over this pH range (Figure 2B). The acidic limb of the bell-shaped pH profile in Figure 2C indicates that an ionization event between pH 5.5 and pH 7 plays an important role in catalysis and may reflect the ionization of the His (pK_a ≈6.1) or Glu (pK_a ≈4.1) zinc ligands. The dramatic effect of pH on the alkaline limb of the profile has previously been associated with a conformational change in eukaryotic TOP (*24*). Given a pH optimum of ≈7.8, we routinely employed a pH of 8 in our kinetic studies.

Tropolysin was potently inhibited by Cbz-$_{(L,D)}$Pheψ(PO_2-CH_2)$_{(L,D)}$Ala-Arg-Tyr, a phosphinic peptide inhibitor that is a potent and specific slow, tight-binding inhibitor of TOP (*13*) (Table 1). A related phosphinic peptide inhibitor of neurolysin, Gly-Pro-$_{(L,D)}$Pheψ(PO_2CH_2)Gly-Pro-Nle, was also a potent tropolysin inhibitor, although 200-fold weaker than Cbz-$_{(L,D)}$Pheψ(PO_2CH_2)$_{(L,D)}$Ala-Arg-Tyr. Metal ion chelators EDTA and 1,10-phenanthroline (although not the non-chelating analogue, 1,7-phenanthroline) were strong inhibitors of tropolysin (Table 1), consistent with tropolysin being a metal-dependent enzyme. Tropolysin was not inhibited by inhibitors of other kininases, including phosphoramidon (an inhibitor of thermoylsin and neprilysin) and thiorphan (an inhibitor of neprilysin), although weak inhibition was observed with captopril (an inhibitor of angiotensin I-converting enzyme, ACE). The thiol-alkylating agents *N*-ethylmaleimide and *p*-(chloromercuri)benzoate were potent inhibitors of tropolysin (Table 1), indicating the presence of one or more free thiol groups in the tropolysin molecule that were required for substrate binding and/or catalysis. This phenomenon has also been reported for TOP (*25*). The crystal structure of TOP has been solved (*26*), and Cys[427], located near the catalytic site, is believed to mediate this inhibition. Cys[427] is conserved in tropolysin (Cys[483]; Figure 1A) and may mediate this inhibition, although this has not been experimentally demonstrated. Interestingly, iodoacetamide, which also reacts with thiol groups in proteins, was a comparatively poor inhibitor of tropolysin activity. Both *p*-(chloromercuri)benzoate and *N*-ethylmaleimide would form large, bulky and charged adducts on a Cys residue, while iodoacetamide would form a small, uncharged adduct. Thus, it seems that a large, bulky charged adduct formed on Cys[483] of tropolysin impairs activity, while a smaller or uncharged adduct would not. Class-specific inhibitors of other peptidases, including DCI, E-64, and pepstatin were without any effect on tropolysin activity (results not shown).

Tropolysin activity was strongly affected by divalent metal cations (Table 2). Zinc was the most potent activator (23-fold) of metal-depleted tropolysin (apotropolysin), with maximal activation observed at 1 μM. These data suggested to us that zinc was the natural cofactor for tropolysin. Indeed, ^{65}Zn has been detected in TOP (*21*). At higher concentrations, zinc was potently inhibitory. Co^{2+} and Mn^{2+} also restored activity to apotropolysin, although at much higher (10−100-fold) concentrations. Furthermore, at high concentrations, Co^{2+} and Mn^{2+} were able to "superactivate" tropolysin, which reached specific activities in excess of what was achievable with zinc. In TOP, this phenomenon has previously been reported for Co^{2+} (*25*). Ca^{2+} and Mg^{2+} were activators of tropolysin activity, while Fe^{2+} and Ni^{2+} ions were potently inhibitory. The pronounced inhibition by Ni^{2+} probably accounts for the poor specific activity we obtained when recombinant tropolysin was purified on Ni^{2+}-agarose, in contrast to the excellent specific activity that eluted from Co^{2+}-agarose.

Tropolysin activity was very sensitive to reducing agents (Figure 3). Native tropolysin purified from *T. brucei brucei* was potently (up to 5-fold) activated by DTT in the concentration range 50−200 μM (Figure 3A). Similarly, reduced glutathione (GSH) maximally activated tropolysin activity at 1 mM. Recombinant tropolysin from both *T. brucei brucei* and *T. brucei rhodesiense* was similarly affected (Figure 3B). TOP is also activated by reducing agents (*25*). This thiol-mediated activation of TOP activity has been attributed to the formation of inactive covalent TOP multimers, which may block access of substrate to the active site (*27*) or may promote a conformational change in the TOP molecule that impairs activity (*28*). Indeed, when purified tropolysin was incubated in the absence of reducing

Table 1: Inhibition of Tropolysin by Synthetic Inhibitors

inhibitor	concn (mM)	relative activity (%)[a] or K_i (nM) purified tropolysin (*T.b.b.*)	recombinant tropolysin (*T.b.b.*)	recombinant tropolysin (*T.b.r.*)
Gly-Pro-$_{(L,D)}$Pheψ(PO_2CH_2)Gly-Pro-Nle[b]		39.7 ± 8.1 (K_i)	58.2 ± 4.6 (K_i)	51.8 ± 7.7 (K_i)
Cbz-$_{(L,D)}$Pheψ(PO_2CH_2)$_{(L,D)}$Ala-Arg-Tyr		0.2 ± 0.1 (K_i)	0.1 ± 0.04 (K_i)	0.1 ± 0.06 (K_i)
1,7-phenanthroline	1.0	97.0 ± 1.2	93.3 ± 4.3	96.6 ± 2.2
1,10-phenanthroline	1.0	0.2 ± 0.0	0.3 ± 0.1	0.2 ± 0.1
EDTA	1.0	32.2 ± 2.1	23.4 ± 1.7	31.8 ± 1.9
iodoacetamide	1.0	84.4 ± 0.9	88.6 ± 1.1	80.7 ± 2.3
N-ethylmaleimide	1.0	22.2 ± 1.4	18.9 ± 1.0	19.7 ± 2.2
p-(chloromercuri)benzoate	0.1	0.9 ± 0.1	0.2 ± 0.0	0.6 ± 0.1
captopril	0.01	78.2 ± 1.9	82.2 ± 1.8	77.5 ± 0.9
thiorphan	0.01	99.1 ± 1.1	98.5 ± 2.2	96.9 ± 3.3
phosphoramidon	0.01	102.2 ± 2.2	99.4 ± 2.4	97.8 ± 1.7

[a] Relative activity represents the activity of an aliquot of TOP preincubated with the respective inhibitor for 5 min, relative to the activity of an aliquot of TOP, preincubated in the absence of inhibitor, but in the same concentration of inhibitor solvent (usually 0.5% dimethyl sulfoxide).[b] Nle, 2-aminohexanoic acid.

Table 2: Reactivation by Divalent Metal Cations of Apotropolysin Purified from *T. brucei brucei*

metal	concn (μM)	specific activity ($\Delta F \cdot s^{-1} \cdot mg^{-1}$)	metal	concn (μM)	specific activity ($\Delta F \cdot s^{-1} \cdot mg^{-1}$)
none		72 ± 8	Fe(II)	1	72 ± 8
Zn(II)	1	1634 ± 277		100	18 ± 4
	10	1088 ± 143	Ca(II)	1	101 ± 3
	100	217 ± 26		100	377 ± 21
	1000	54 ± 11	Mg(II)	1	127 ± 42
Co(II)	1	729 ± 44		100	191 ± 18
	10	1408 ± 119	Ni(II)	1	88 ± 17
	100	2232 ± 125		100	29 ± 19
Mn(II)	1	886 ± 12			
	10	1918 ± 119			
	100	2902 ± 209			

agents, multimer formation was observed, since a protein peak devoid of catalytic activity was eluted from a molecular exclusion chromatography column at approximately 180 kDa. After reduction with 100 μM DTT, activity was detected against Mca-(Ala^7,Lys(Dnp)^9)-BK (Figure 3C). These data indicate that tropolysin does form multimers under nonreducing conditions. In TOP, multimer formation is believed to be mediated by a tight cluster of three solvent-accessible Cys residues (Cys^{246}, Cys^{248}, and Cys^{253}) (*27*) and also by Cys^{46}, Cys^{682}, and Cys^{687} (*28*). Interestingly, none of these cysteine residues are conserved in tropolysin (Figure 1A). However, tropolysin does contain 13 Cys residues (circled in Figure 1A), three of which are located in the disordered N-terminus of the molecule and are (by analogy with TOP) likely to be solvent accessible (*26*) and, thus, in a position to mediate multimer formation. Indeed, at least one Cys residue in the disordered N-terminus of TOP is believed to mediate thiol activation (*28*).

Higher concentrations of reducing agents (>250 μM DTT or >1 mM GSH; Figure 3A) inhibited tropolysin activity. This may be attributed either to the disruption of intramolecular disulfide bridges or to the high thiophilicity of the catalytic zinc atom. Since TOP does not contain any disulfide bridges (*26*), and replacement of the highly thiophilic Zn^{2+} with the less thiophilic Mn^{2+} in TOP reduced the degree of inhibition observed with DTT (*15*), it is probable that the inhibition of tropolysin results from a direct interaction between DTT and the catalytic zinc atom.

Interestingly, oligopeptidase B, a serine oligopeptidase from African trypanosomes, is also activated by reducing agents in the low millimolar range (*29*). The trypanosome cytosol is a strongly reducing environment, and total cytosolic GSH concentrations are in the region of 1 mM (*29*). In Figure 3A (inset), we illustrate that this is the optimal GSH concentration for maximal activation of tropolysin. These data raise the possibility that the activity of both tropolysin and OpdB is regulated by intracellular reducing agents in the cytosol of African trypanosomes.

Substrate Specificity of Tropolysin. The substrate specificity of tropolysin was explored with a series of intramolecularly quenched fluorogenic substrates based on the core BK sequence of the general formula *o*-aminobenzoyl (Abz)-Gly-Phe-Ser-Pro-Phe-Arg-Gln-2,4-ethylenediamine (EDDnp) (*14*). The hydrolysis data are summarized in Table 3, and the conclusions drawn from those data are summarized in Figure 4. The Abz-**Gly**^{1}-Phe^2-Ser^3-Pro^4-Phe^5-Arg^6-Gln^7-2,4-EDDnp peptide was hydrolyzed exclusively at the Pro^4↓Phe^5 bond by tropolysin (Tables 3 and S2; see Supporting Information). Similarly, when Gly^1 was replaced with Glu, Ser, Gly, and Phe, cleavage was observed only at Pro^4↓Phe^5. The lowest K_m and the highest k_{cat}/K_m were observed with Glu in position 1 (Table S2), suggesting a P_4 substrate preference of Glu > (Ser, Gly) > Phe for this substrate. When the carboxylic acid side chain of Glu^1 was replaced with an uncharged amine (Gln or Asn), the K_m was elevated 3-fold, and the k_{cat}/K_m dropped 2-fold. Furthermore, cleavage was now evident at two sites in the peptide, Pro^4↓Phe^5 and Phe^2↓Ser^3, although the Pro^4↓Phe^5 cleavage was the predominant cleavage. An elevated K_m and secondary cleavages were also observed when Glu^1 was replaced with Leu, Ala, and Ile. We surmise from these data that tropolysin best accommodates large acidic side chains in P_4. This represents a major substrate specificity shift from TOP and neurolysin, which do not demonstrate a particular preference for acidic side chains in the P_4 position (*14*). The crystal structure of TOP (*26*) has implicated His^{495} in the substrate-binding loop of TOP in recognition of the substrate P_4 residue (see Figure 4). In tropolysin, this residue is replaced by the more basic Arg^{553} (Figure 1C), which may account for the increased specificity for an acidic residue in P_4 in tropolysin.

When Phe^2 of the substrate Abz-Gly^1-**Phe**^{2}-Ser^3-Pro^4-Phe^5-Arg^6-Gln^7-EDDnp was replaced with a variety of residues, a single cleavage at Pro^4↓Phe^5 was observed (Tables 3 and S3), with Pro and bulky hydrophobic residues (Phe) best

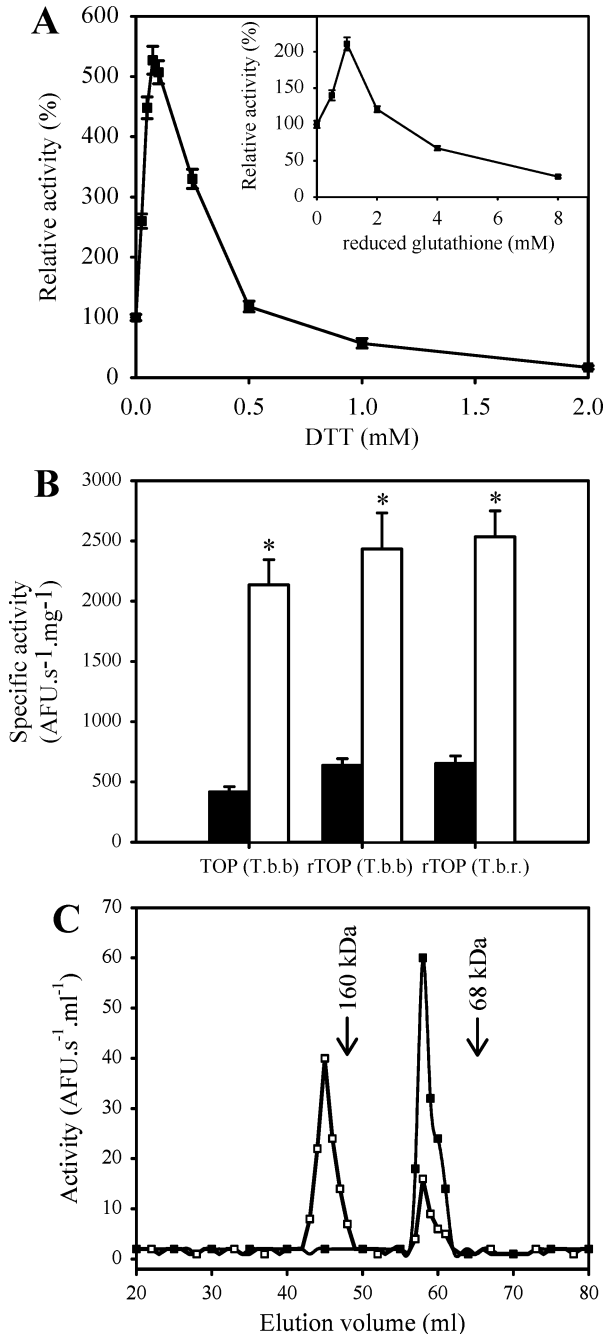

FIGURE 3: Reductive activation of tropolysin. (A) Native tropolysin purified from *T. brucei brucei* was incubated in DTT-free buffer (5 mM Tris-HCl, 100 mM NaCl, 10 mM $CaCl_2$, pH 8) for 24 h at 4 °C to promote inactivation, after which tropolysin was preincubated (5 min, 37 °C) in the presence of DTT (0−2 mM) or reduced glutathione (GSH, 0−8 mM, inset) prior to the addition of Mca-(Ala^7,Lys(Dnp)^9)-BK substrate, from which the specific activity was determined. (B) The activation of native *T. brucei brucei* tropolysin and recombinant tropolysin from *T. brucei brucei* and *T. brucei rhodesiense* was studied as described for (A), in the absence (closed bars) and presence (open bars) of 100 μM DTT. Data represent the mean specific activity ± SD ($n = 3$). *, $P < 0.001$ between treated and untreated groups. (C) To determine whether tropolysin formed multimers under nonreducing conditions, tropolysin was incubated (24 h, 4 °C) in 50 mM Tris-HCl, 100 mM NaCl, and 10 mM $CaCl_2$, pH 8, in either the presence (■) or absence (□) of 100 μM DTT. Samples were resolved by passage over a Sephacryl S-200 HR column (1250 × 15 mm, 0.24 mL·min^{-1}) equilibrated in 50 mM Tris-HCl, 100 mM NaCl, and 10 mM $CaCl_2$, pH 8, in the presence (■) or absence (□) of 100 μM DTT. In both instances, column fractions were reduced with 100 μM DTT prior to assaying hydrolytic activity against Mca-(Ala^7,Lys(Dnp)^9)-BK.

Table 3: Hydrolysis of Peptides of the General Formula Abz-GFSPFRQ-EDDnp at the P↓F Bond by Recombinant Tropolysin from *T. brucei brucei*

amino acid	k_{cat}^{PF}/K_m ($s^{-1}\cdot\mu M^{-1}$) for amino acid at position[a]					
	P_4	P_3	P_1	P_1'	P_2'	P_3'
Ala	3.0	1.4	nd	nd	2.6	nd
Arg	nd	nd	3.6	0.5	3.7	0.7
Asn	4.6	1.6	nd	1.3	nd	nd
Asp	nd	1.6	nd	0.1	nd	nd
Gln	2.2	nd	4.5	nd	nd	3.0
Glu	8.3	nd	0.8	nd	nd	nd
Gly	3.7	nd	nd	nd	nd	nd
His	nd	nd	3.1	0.7	1.6	nd
Ile	2.9	nd	nd	nd	nd	nd
Leu	2.7	2.3	nd	nd	1.8	6.4
Phe	3.2	3.1	5.0	3.7	nd	nd
Pro	nd	3.0	3.7	nd	0.5	nd
Ser	4.7	1.7	2.5	nd	0.5	1.5

[a] nd, no hydrolysis detected.

accommodated in P_3, which is similar to what is observed with TOP (*14*). However, acidic residues were also accommodated in P_3, in strong contrast to TOP, where they are very poorly tolerated (*14*). This accommodation of acidic residues in P_3 (and P_4, described above) is probably attributable to the higher incidence of basic amino acid side chains in the substrate-binding loop of tropolysin (Figure 4). In addition to the His → Arg substitution, several other replacements are observed in the substrate-binding loop of tropolysin. Most notably, Glu^{497} in TOP is replaced with Lys^{555} in tropolysin, and Glu^{487} in TOP is replaced with Lys^{545} in tropolysin (Figures 1C and 4). These replacements are significant because they both exchange acidic for basic residues. Similarly, Gln^{485} in TOP is replaced with Arg^{543} in tropolysin (Figures 1C and 4). Thus, the area of the substrate-binding loop in tropolysin that recognizes the P_3 and P_4 substrate residues is very basic compared to TOP, probably accounting for the preference for acidic side chains in P_3 and P_4.

When Pro^4 of the substrate Abz-Gly^1-Phe^2-Ser^3-**Pro**^{4}-Phe^5-Arg^6-Gln^7-EDDnp was replaced with a variety of residues, a single cleavage at Xaa^4↓Phe5 was exclusively observed (Tables 3 and S4), with large bulky hydrophobic residues (Phe), and other large residues Gln and Pro best accommodated in P_1, which is similar to what is observed with TOP (*14*). Electrostatic interactions did not appear to play a significant role in P_1 recognition, because, despite the high incidence of basic residues in the tropolysin substrate-recognition loop, acidic residues (Glu) were not favored in P_1.

When Phe^5 of the substrate Abz-Gly^1-Phe^2-Ser^3-Pro^4-**Phe**^{5}-Arg^6-Gln^7-EDDnp was replaced with an uncharged (Asn) residue, a single cleavage at Pro^4↓Xaa^5 was exclusively observed, in the case of both Phe and Asn in position 5 (Tables 3 and S5), indicating a preference for hydrophobic or large, uncharged residues in P_1'. However, when Phe^5 was replaced with charged residues (His, Arg, or Asp) cleavage was evident at two sites in the peptide, Pro^4↓Xaa^5 and Phe^2↓Ser^3, with the Phe^2↓Ser^3 cleavage predominant. We surmised from these data that charged residues were not preferred in P_1'. In particular, the charged residues Arg and Asp were not tolerated in P_1', elevating the K_m 3−4-fold. In TOP, Glu^{469} is implicated in recognition of the substrate P_1'

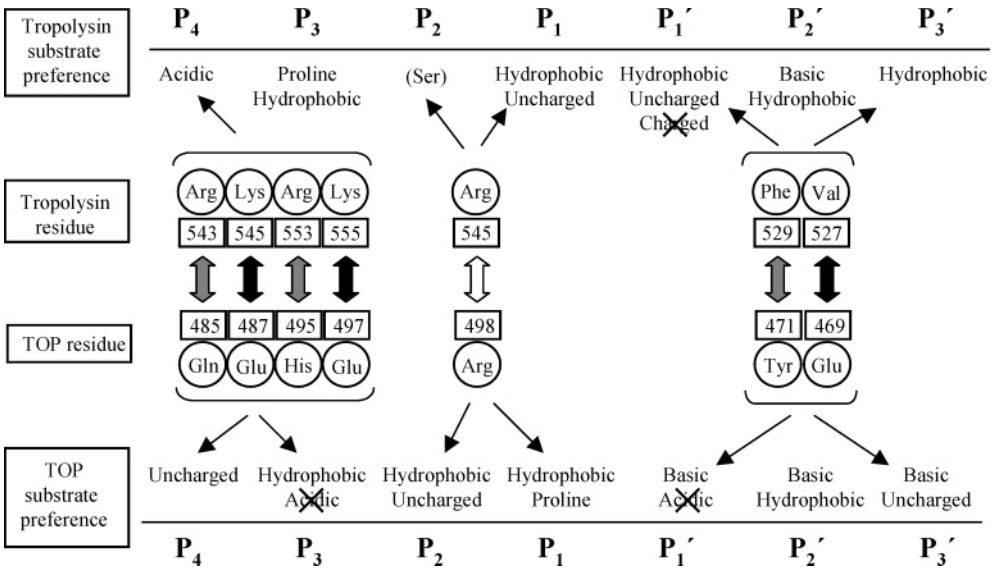

FIGURE 4: Structural framework comparing the interactions of the S_4-S_3' regions of tropolysin and TOP. The substrate specificity of tropolysin over residues P_4-P_3', experimentally determined in this study (Tables 3 and S2−S7), is summarized at the top of the figure. Key residues of tropolysin and TOP that mediate interactions with P_4-P_3' substrate residues are indicated, along with their numbering in the primary sequences from *T. brucei brucei* (for tropolysin) and *H. sapiens* (for TOP). Key residues conserved between the two enzymes are indicated with a white double-headed arrow. Nonconserved residues are indicated with a gray double-headed arrow when replacements cause a mild change in the physicochemical properties of the residue, while dramatic changes (such as a charge reversal) are indicated with a black double-headed arrow. The residue preferences for TOP are indicated at the bottom of the figure (from refs *14* and *26*). Where residues are not tolerated, they are crossed out. TOP, thimet oligopeptidase.

and P_3' residues (*26*). In tropolysin, Glu^{469} is replaced with a Val residue (Figures 1C and 4). Furthermore, nearby Tyr^{471} (in TOP) is replaced with Phe in tropolysin. Thus, the P_1' (and perhaps P_3') recognition area of the tropolysin substrate-binding loop is more hydrophobic in character than TOP. This perhaps accounts for the poor accommodation of highly charged residues in P_1'. This represents another difference in substrate specificity when compared with TOP, where the side chains of the basic residues His and Arg (but not acidic residues; see Figure 4) are the preferred residues in P_1' (*14*).

When Arg^6 of the substrate Abz-Gly^1-Phe^2-Ser^3-Pro^4-Phe^5-**Arg^6**-Gln^7-EDDnp was replaced with other basic (His) or hydrophobic (Ala) residues, a single cleavage at $Pro^4\downarrow Phe^5$ was exclusively observed (Tables 3 and S6), indicating a preference for basic or hydrophobic residues in P_2'. However, when Arg^6 was replaced with Ser or Pro, cleavage was evident at two sites in the peptide, $Pro^4\downarrow Phe^5$ and $Phe^2\downarrow Ser^3$, with the $Phe^2\downarrow Ser^3$ cleavage predominant with the Ser substitution and equivalent with the Pro substitution. Thus, the P_2' preference appears to be relatively unselective and parallels the specificity of TOP (*14*). The presence of several acidic residues in the P′ recognition area of the TOP substrate-binding loop (Asp^{524}, Asp^{525}; Figure 1C) may account for the slight preference for basic residues in P2′, but this would not explain the accommodation of hydrophobic residues in P_2' as well.

When Gln^7 of the substrate Abz-Gly^1-Phe^2-Ser^3-Pro^4-Phe^5-Arg^6-**Gln^7**-EDDnp was replaced with hydrophobic (Leu) or small (Gly) residues, a single cleavage at $Pro^4\downarrow Phe^5$ was observed exclusively (Tables 3 and S7). A Leu replacement yielded the lowest K_m and highest k_{cat}/K_m, indicating that large, hydrophobic side chains were preferred in P_3'. This contrasts with TOP, where basic amino acid side chains such as Arg are best accommodated in P_3'. In TOP, Glu^{469} is implicated in recognition of the substrate P_3' (as well as P_1') residues (*26*) and most likely electrostatically interacts with the P_3' residue, hence the preference for Arg in P_3' by TOP. In tropolysin this Glu residue is replaced with a Val residue (Figures 1C and 4). Thus, the P_3' recognition area of the tropolysin substrate-binding loop is more hydrophobic in character than TOP, hence the preference for Leu in P_3'. In support of this idea, when Phe^5 was replaced with charged residues (His, Arg, or Asp; Table S5), cleavage was evident at two sites in the peptide, $Pro^4\downarrow Phe^5$ and $Phe^2\downarrow Ser^3$, and cleavage occurred at equivalent rates. In both cases, Arg (or another charged residue) would be present in P_3', probably accounting for the equivalent rate of hydrolysis of the $Pro^4\downarrow Phe^5$ and $Phe^2\downarrow Ser^3$ bonds.

The substrate specificity of tropolysin is summarized in Figure 4, together with putative interactions between key determinants of substrate specificity. The preponderance of basic residues in the P_4 binding region directs specificity for acidic residues in P_4, in contrast to TOP, where they are not tolerated, because the TOP P_4 binding region is acidic. The tropolysin P′ binding region has hydrophobic characteristics, directing specificity for hydrophobic residues in P_1, P_1', and P_2'. Again, this contrasts with TOP, where a preponderance of charged and acidic residues direct specificity for basic side chains in P_1' and P_3'. Taken together, these data suggest that tropolysin exhibits a distinct substrate specificity when compared to TOP and neurolysin. While we propose that some of these differences in substrate specificity may be mediated by nonconservative replacements of key substrate-recognizing side chains, these replacements still cannot explain all of the substrate specificity differences that we observed. A crystal structure of tropolysin in a complex with peptide substrates will be required to resolve the structural basis underlying this altered substrate specificity of tropolysin.

Cleavage of Vasoactive Peptides by Tropolysin. The vasoactive kinins BK and kallidin (Lys-BK) were cleaved by recombinant tropolysin with a k_{cat} of 80−120 s^{-1} and a

Table 4: Hydrolysis of Vasoactive Kinins by Tropolysin Purified from *T. brucei brucei*

peptide	K_m (μM)	k_{cat} (s^{-1})	k_{cat}/K_m ($s^{-1}\cdot\mu M^{-1}$)
bradykinin	32 ± 19	79 ± 41	2.5
kallidin	56 ± 28	119 ± 39	2.1
angiotensin I	92 ± 23	28 ± 21	0.3
angiotensin II	nd	nd	nd

[a] nd, no hydrolysis detected.

K_m of 30−50 μM ($k_{cat}/K_m \approx 2.3\ s^{-1}\cdot\mu M^{-1}$; Table 4). Thus, both naturally occurring kinins were excellent substrates of tropolysin, confirming that tropolysin is indeed a kininase. Furthermore, angiotensin I (AngI) was cleaved by tropolysin, although hydrolysis was not as efficient as that observed for the kinins ($k_{cat}/K_m \approx 0.3\ s^{-1}\cdot\mu M^{-1}$; Table 4). Angiotensin II was not cleaved by tropolysin (Table 4). To confirm that bacterial peptidases carried over in trace amounts from the hyperexpression procedure were not responsible for the observed activity against regulatory peptides, a catalytically inactive tropolysin was prepared by converting the essential catalytic Glu^{532} residue (equivalent to Glu^{474} in TOP; Figure 1C) to a Gln residue. This conversion has been shown to yield a catalytically inactive TOP molecule (*21*, *22*). Reaction products were then analyzed by MALDI-TOF mass spectrometry. When BK was incubated with catalytically inactive recombinant tropolysin(E532Q) at a 1:200 (mol/mol; by mass/mass) tropolysin:BK ratio for 30 min, a single product corresponding to intact BK was detected (*m*/*z* $[M + H]^+$ calculated 1059.56, found 1060.42; Figure 5A). However, upon incubation with wild-type recombinant tropolysin, two peptide products were identified as BK(1−5) (*m*/*z* $[M + H]^+$ calculated 572.31, found 572.84) and BK(6−9) (*m*/*z* $[M + H]^+$ calculated 505.27, found 505.77) (Figure 5B). Similarly, when kallidin was incubated with catalytically inactive recombinant tropolysin(E532Q) at a 1:200 (mol/mol; by mass/mass) tropolysin:kallidin ratio for 30 min, a single product corresponding to intact kallidin (*m*/*z* $[M + H]^+$ calculated 1187.66, found 1188.46) was observed, while catalytically active recombinant tropolysin generated two fragments: kallidin(1−6) (*m*/*z* $[M + H]^+$ calculated 700.40, found 700.91) and kallidin(7−10) (*m*/*z* $[M + H]^+$ calculated 505.27, found 505.59) (spectra not shown). When AngI was incubated with catalytically inactive recombinant tropolysin-(E532Q) at a 1:100 (mol/mol; by mass/mass) tropolysin:AngI ratio for 30 min, a single product corresponding to intact AngI was detected (*m*/*z* $[M + H]^+$ calculated 1295.68, found 1296.44; Figure 5C). However, upon incubation with catalytically active recombinant tropolysin, two peptide products with specific *m*/*z* values for AngI(1−7) (*m*/*z* $[M + H]^+$ calculated 898.47, found 899.09) and AngI(8−10) (*m*/*z* $[M + H]^+$ calculated 415.22, found 415.57) were observed (Figure 5D). Thus, tropolysin cleaved BK and kallidin exclusively at the Phe↓Ser bond and AngI at the Pro↓Phe bond.

Interestingly, our BK-derived fluorescent peptide substrates (Abz-GFSPFRQ-EDDnp) were generally cleaved at the Pro↓Phe bond (Tables S2−S7), although the native BK peptide (RPPGFSPFR) was cleaved exclusively at the Phe↓Ser bond (Table 4 and Figure 5). These data indicate that the N-terminal Arg^1-Pro^2-Pro^3 of BK may contain additional recognition elements for tropolysin that are not present in the fluorogenic peptide, which promote preferential cleavage at the Phe↓Ser bond. Indeed, Met^{490} in TOP (equivalent to Thr^{548} in tropolysin; Figure 1C) is implicated

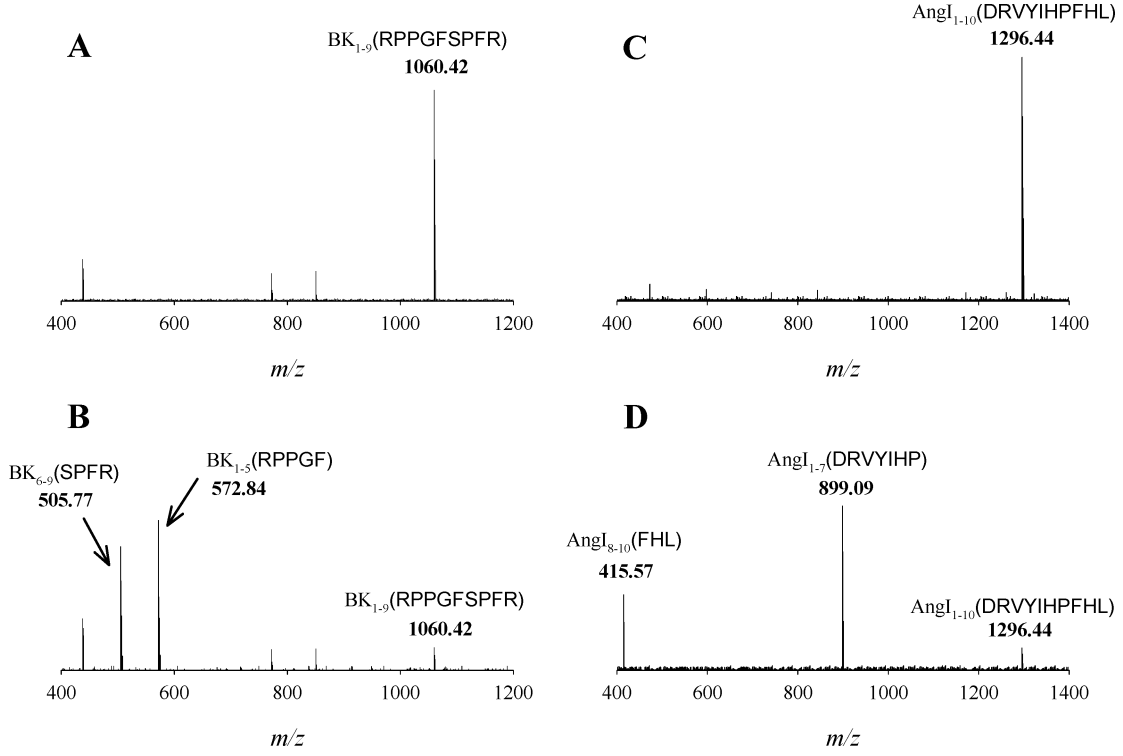

FIGURE 5: Degradation of regulatory peptides by tropolysin. BK was preincubated with catalytically inactive recombinant tropolysin-(E532Q) (A) or catalytically active recombinant tropolysin (B) at 1:250 [mol/mol, by mass/mass for tropolysin(E532Q) and by activity/mass for tropolysin] tropolysin:BK ratios for 30 min at 37 °C. In a second set of reactions, AngI was preincubated with catalytically inactive tropolysin(E532Q) (C) or catalytically active tropolysin (D) at 1:250 [mol/mol, by mass/mass for tropolysin(E532Q) and by activity/mass for tropolysin] tropolysin:BK ratios for 30 min at 37 °C, after which reaction products were analyzed by MALDI-TOF mass spectrometry.

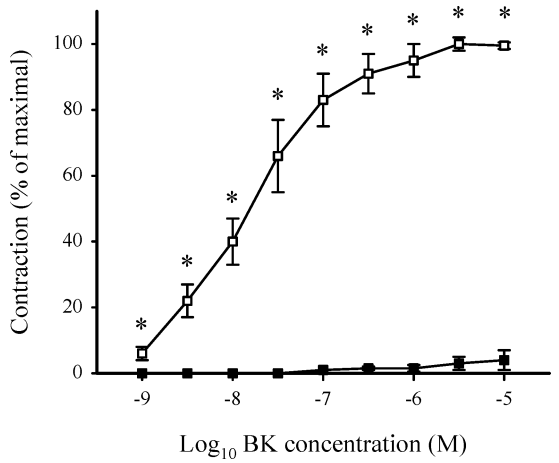

FIGURE 6: Tropolysin abrogates BK B_2 receptor stimulation by BK. BK was preincubated with catalytically active recombinant tropolysin (■) or catalytically inactive recombinant tropolysin-(E532Q) (□) at 1:50 [mol/mol, by activity/mass for tropolysin and by mass/mass for tropolysin(E532Q)] tropolysin:BK ratios for 30 min at 37 °C and applied to ileum segments, as described in the Experimental Procedures. Data represent the mean percentage of maximal contraction ± SD ($n = 3$). *, $P < 0.01$ between ■ and □ groups at the same BK concentration.

in recognition of the P_7 residue in substrate peptides (*26*). Thus, additional recognition elements exist in tropolysin that would not be detected with our fluorogenic peptides, which are too short to facilitate P_7-S_7 interaction. Furthermore, TOP does not cleave the two C-terminal peptide bonds in a peptide (*30*). In native BK, the Pro−Phe bond is located in this excluded region, while in our fluorogenic peptides, the addition of a C-terminal Gln residue places the Pro−Phe bond in the included region of the peptide.

Cleavage by Tropolysin Abrogates BK Biological Activity. Incubation of BK with recombinant tropolysin at 1:50 (mol/mol; by activity/mass) tropolysin:BK ratios for 1 h abrogated BK B_2 receptor stimulation by BK, as judged by the contractile response of the guinea pig ileum (Figure 6). In contrast, incubation at the same ratios with catalytically inactive recombinant tropolysin(E532Q) preserved the BK B_2 receptor stimulation properties of BK (Figure 6). Neither recombinant tropolysin nor catalytically inactive recombinant tropolysin(E532Q) possessed intrinsic ileum-contracting activity (data not shown). These data indicate that tropolysin can destroy the BK B_2 receptor-stimulating properties of BK and are consistent with reports that BK B_2 receptor stimulation requires the presence of both Arg^1 and Arg^9 in the same BK molecule (*19*), in contrast to BK B_1 receptor stimulation, and other BK-mediated processes, in which BK degradation products may participate (*19*). Since the guinea pig ileum assay exclusively measures responses mediated by the BK B_2 receptors, a more meaningful measure of BK activity is obtained in a live animal model of BK-induced hypotension. The prohypotensive properties of BK were abrogated after incubation with catalytically active recombinant tropolysin (Figure 7) at 1:50 (mol/mol; by activity/mass) tropolysin:BK ratios for 1 h, while incubation at the same ratios with recombinant catalytically inactive tropolysin(E532Q) did not impair the prohypotensive properties of BK. Neither recombinant tropolysin nor catalytically inactive recombinant tropolysin(E532Q) possessed intrinsic prohypotensive activity (Figure 7). Together, these data suggest that the degradation of vasoactive kinins by tropolysin destroys the biological activity of these kinins.

Tropolysin in Perspective. The peptidases of parasitic protozoans are currently the subject of considerable interest, in the hope of identifying novel virulence factors, drug targets, and vaccine candidates. To date, our knowledge of the peptidolytic capacity of African trypanosomes has been limited to four peptidases. We report here the purification, cloning, and biochemical characterization of tropolysin, a new peptidase from two highly pathogenic African trypanosomes. This peptidase, which is a new member of the M3A family of metallopeptidases, displays a unique substrate specificity compared with its eukaryotic relatives, and this is the first report of any member of the M3 family of metallopeptidases from any protozoan organism.

We document in this study that tropolysin has potent kininase activity, and this may have relevance to the pathogenesis of African trypanosomiasis. The kallikrein−kinin system is severely dysregulated in trypanosome-

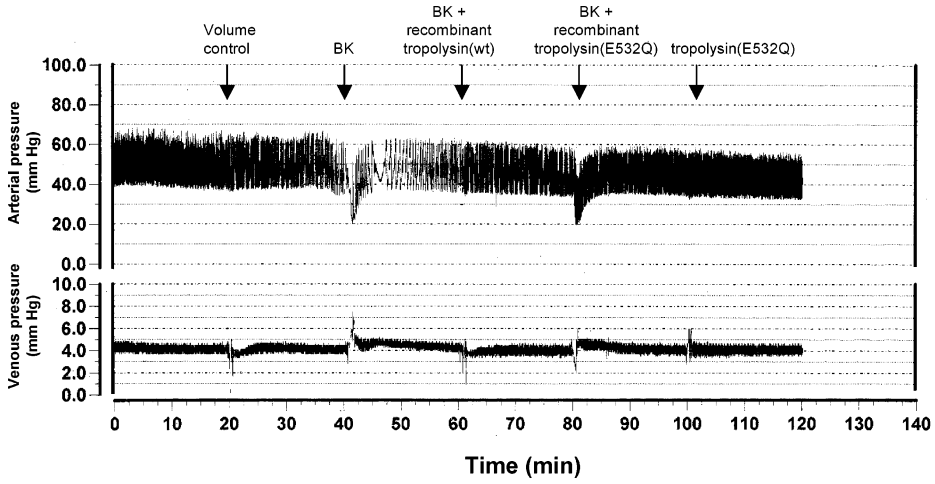

FIGURE 7: Tropolysin abrogates the prohypotensive properties of BK. Agents were applied as a bolus over 30 s directly to the venous circulation of an anesthetized rabbit via the right ear vein, as indicated, while mean arterial and venous pressures were continuously monitored by catheters in the left carotid artery and right ear vein. At 20 min intervals agents were applied (indicated above the arterial pressure trace) as described in the Experimental Procedures. Data presented are for a single rabbit but are representative of data from three other rabbits. The spikes on the venous pressure traces occur during the administration of the agents since they are administered via the pressure sensor catheter and thus do not indicate changes to venous pressure.

infected hosts (*31*), which is thought to contribute to vascular lesions observed in African trypanosomiasis (*32*). Upon release by dead or dying trypanosomes in the host bloodstream, tropolysin would be in an excellent position to influence the activity of host vasoactive kinins, similar to what has been described for OpdB (*33*). Other investigators have suggested that, in addition to OpdB, a trypanosome-derived "cation-sensitive, thiol-dependent peptidase" is active in the plasma of infected hosts (*12*). In this study, we describe exactly this type of peptidase, since tropolysin is both cation sensitive and thiol dependent. Studies on the possible role of tropolysin in modulating regulatory peptide dynamics in the plasma of trypanosome-infected hosts are currently underway in our laboratories. Furthermore, other oligopeptidases from trypanosomes have also received attention as candidate therapeutic targets (*5*, *10*, *11*), and since TOP in mammals plays a key role in intracellular protein turnover, tropolysin may represent an attractive chemotherapeutic target in trypanosomes.

ACKNOWLEDGMENT

We thank Dr. Oliver Eickelberg for outstanding support and Dr. Alan J. Barrett and Dr. Neil D. Rawlings for very helpful discussions that pertained to the phylogenetic relationships of peptidases and their nomenclature. The table of contents artwork photograph is by Sinclair Stammers, available courtesy of WHO/TDR/Stammers.

SUPPORTING INFORMATION AVAILABLE

Purification table for the isolation of tropolysin from *T. brucei brucei* lysates (Table S1), documentation of the purity of the tropolysin preparations, as well as the analysis of gene copy number and expression of the *trn* gene in different trypanosome life-cycle stages (Figure S1), and raw kinetic data for the hydrolysis of substituted fluorogenic peptides by recombinant tropolysins from *T. brucei brucei* and *T. brucei rhodesiense* and by native tropolysin from *T. brucei brucei* (Tables S2−S7). This material is available free of charge via the Internet at http://pubs.acs.org.

REFERENCES

1. Barrett, M. P., Burchmore, R. J., Stich, A., Lazzari, J. O., Frasch, A. C., Cazzulo, J. J., and Krishna, S. (2003) The trypanosomiases, *Lancet 362*, 1469−1480.
2. Klemba, M., and Goldberg, D. E. (2002) Biological roles of proteases in parasitic protozoa, *Annu. Rev. Biochem. 71*, 275−305.
3. Santana, J. M., Grellier, P., Schrével, J., and Teixeira, A. R. (1997) A *Trypanosoma cruzi*-secreted 80 kDa proteinase with specificity for human collagen types I and IV, *Biochem. J. 325*, 129−137.
4. Caler, E. V., Vaena de Avalos, S., Haynes, P. A., Andrews, N. W., and Burleigh, B. A. (1998) Oligopeptidase B-dependent signaling mediates host cell invasion by *Trypanosoma cruzi*, *EMBO J. 17*, 4975−4986.
5. Joyeau, R., Maoulida, C., Guillet, C., Frappier, F., Teixeira, A. R., Schrével, J., Santana, J., and Grellier, P. (2000) Synthesis and activity of pyrrolidinyl- and thiazolidinyl-dipeptide derivatives as inhibitors of the Tc80 prolyl oligopeptidase from *Trypanosoma cruzi*, *Eur. J. Med. Chem. 35*, 257−266.
6. Grellier, P., Vendeville, S., Joyeau, R., Bastos, I. M., Drobecq, H., Frappier, F., Teixeira, A. R., Schrével, J., Davioud-Charvet, E., Sergheraert, C., and Santana, J. M. (2001) *Trypanosoma cruzi* prolyl oligopeptidase Tc80 is involved in nonphagocytic mammalian cell invasion by trypomastigotes, *J. Biol. Chem. 276*, 47078−47086.
7. Morty, R. E., Lonsdale-Eccles, J. D., Morehead, J., Caler, E. V., Mentele, R., Auerswald, E. A., Coetzer, T. H., Andrews, N. W., and Burleigh, B. A. (1999) Oligopeptidase B from *Trypanosoma brucei*, a new member of an emerging subgroup of serine oligopeptidases, *J. Biol. Chem. 274*, 26149−26156.
8. Morty, R. E., Authié, E., Troeberg, L., Lonsdale-Eccles, J. D., and Coetzer, T. H. (1999) Purification and characterisation of a trypsin-like serine oligopeptidase from *Trypanosoma congolense*, *Mol. Biochem. Parasitol. 102*, 145−155.
9. Morty, R. E., Pellé, R., Vadász, I., Uzcanga, G. L., Seeger, W., and Bubis, J. (2005) Oligopeptidase B from *Trypanosoma evansi*: a parasite peptidase that inactivates atrial natriuretic factor in the bloodstream of infected hosts, *J. Biol. Chem. 280*, 10925−10937.
10. Morty, R. E., Troeberg, L., Pike, R. N., Jones, R., Nickel, P., Lonsdale-Eccles, J. D., and Coetzer, T. H. (1998) A trypanosome oligopeptidase as a target for the trypanocidal agents pentamidine, diminazene and suramin, *FEBS Lett. 433*, 251−256.
11. Morty, R. E., Troeberg, L., Powers, J. C., Ono, S., Lonsdale-Eccles, J. D., and Coetzer, T. H. (2000) Characterisation of the antitrypanosomal activity of peptidyl alpha-aminoalkyl phosphonate diphenyl esters, *Biochem. Pharmacol. 60*, 1497−1504.
12. Tetaert, D., Soudan, B., Huet-Duvillier, G., Degand, P., and Boersma, A. (1993) Unusual cleavage of peptidic hormones generated by trypanosome enzymes released in infested rat serum, *Int. J. Pept. Protein Res. 41*, 147−152.
13. Jiráček, J., Yiotakis, A., Vincent, B., Lecoq, A., Nicolaou, A., Checler, F., and Dive, V. (1995) Development of highly potent and selective phosphinic peptide inhibitors of zinc endopeptidase 24−15 using combinatorial chemistry, *J. Biol. Chem. 270*, 21701−21706.
14. Oliveira, V., Campos, M., Melo, R. L., Ferro, E. S., Camargo, A. C., Juliano, M. A., and Juliano, L. (2001) Substrate specificity characterization of recombinant metallo oligo-peptidases thimet oligopeptidase and neurolysin, *Biochemistry 40*, 4417−4425.
15. Barrett, A. J., and Brown, M. A. (1990) Chicken liver Pz-peptidase, a thiol-dependent metallo-endopeptidase, *Biochem. J. 271*, 701−706.
16. Oliveira, V., Gatti, R., Rioli, V., Ferro, E. S., Spisni, A., Camargo, A. C., Juliano, M. A., and Juliano, L. (2002) Temperature and salts effects on the peptidase activities of the recombinant metallooligopeptidases neurolysin and thimet oligopeptidase,*Eur. J. Biochem. 269*, 4326−4334.
17. Morty, R. E., and Morehead, J. (2002) Cloning and characterization of a leucyl aminopeptidase from three pathogenic *Leishmania* species, *J. Biol. Chem. 277*, 26057−26065.
18. Del Nery, E., Juliano, M. A., Lima, A. P., Scharfstein, J., and Juliano, L. (1997) Kininogenase activity by the major cysteinyl proteinase (cruzipain) from *Trypanosoma cruzi*, *J. Biol. Chem. 272*, 25713−25718.
19. Skidgel, R. A. (1992) Bradykinin-degrading enzymes: structure, function, distribution, and potential roles in cardiovascular pharmacology, *J. Cardiovasc. Pharmacol. 20* (Suppl. 9), S4−S9.
20. El-Sayed, N. M., Alarcon, C. M., Beck, J. C., Sheffield, V. C., and Donelson, J. E. (1995) cDNA expressed sequence tags of *Trypanosoma brucei rhodesiense* provide new insights into the biology of the parasite, *Mol. Biochem. Parasitol. 73*, 75−90.
21. Chen, J. M., Stevens, R. A., Wray, P. W., Rawlings, N. D., and Barrett, A. J. (1998) Thimet oligopeptidase: site-directed mutagenesis disproves previous assumptions about the nature of the catalytic site, *FEBS Lett. 435*, 16−20.
22. Cummins, P. M., Pabon, A., Margulies, E. H., and Glucksman, M. J. (1999) Zinc coordination and substrate catalysis within the neuropeptide processing enzyme endopeptidase EC 3.4.24.15. Identification of active site histidine and glutamate residues, *J. Biol. Chem. 274*, 16003−16009.
23. Oliveira, V., Araujo, M. C., Rioli, V., de Camargo, A. C., Tersariol, I. L., Juliano, M. A., Juliano, L., and Ferro, E. S. (2003) A structure-based site-directed mutagenesis study on the neurolysin (EC 3.4.24.16) and thimet oligopeptidase (EC 3.4.24.15) catalysis, *FEBS Lett. 541*, 89−92.
24. Sigman, J. A., Edwards, S. R., Pabon, A., Glucksman, M. J., and Wolfson, A. J. (2003) pH dependence studies provide insight into the structure and mechanism of thimet oligopeptidase (EC 3.4.24.15), *FEBS Lett. 545*, 224−228.
25. Orlowski, M., Reznik, S., Ayala, J., and Pierotti, A. R. (1989) Endopeptidase 24.15 from rat testes. Isolation of the enzyme and its specificity toward synthetic and natural peptides, including enkephalin-containing peptides, *Biochem. J. 261*, 951−958.

26. Ray, K., Hines, C. S., Coll-Rodriguez, J., and Rodgers, D. W. (2004) Crystal structure of human thimet oligopeptidase provides insight into substrate recognition, regulation, and localization, *J. Biol. Chem. 279*, 20480−20489.
27. Shrimpton, C. N., Glucksman, M. J., Lew, R. A., Tullai, J. W., Margulies, E. H., Roberts, J. L., and Smith, A. I. (1997) Thiol activation of endopeptidase EC 3.4.24.15. A novel mechanism for the regulation of catalytic activity, *J. Biol. Chem. 272*, 17395−17399.
28. Sigman, J. A., Sharky, M. L., Walsh, S. T., Pabon, A., Glucksman, M. J., and Wolfson, A. J. (2003) Involvement of surface cysteines in activity and multimer formation of thimet oligopeptidase, *Protein Eng. 16*, 623−628.
29. Morty, R. E., Shih, A. Y., Fülöp, V., and Andrews, N. W. (2005) Identification of the reactive cysteine residues in oligopeptidase B from *Trypanosoma brucei*, *FEBS Lett. 579*, 2191−2196.
30. Camargo, A. C., Gomes, M. D., Reichl, A. P., Ferro, E. S., Jacchieri, S., Hirata, I. Y., and Juliano, L. (1997) Structural features that make oligopeptides susceptible substrates for hydrolysis by recombinant thimet oligopeptidase, *Biochem. J. 324*, 517−522.
31. Veenendaal, G. H., van Miert, A. S., van den Ingh, T. S., Schotman, A. J., and Zwart, D. (1976) A comparison of the role of kinins and serotonin in endotoxin induced fever and *Trypanosoma vivax* infections in the goat, *Res. Vet. Sci. 21*, 271−279.
32. Goodwin, L. G., and Hook, S. V. (1968) Vascular lesions in rabbits infected with *Trypanosoma (Trypanozoon) brucei*, *Br. J. Pharmacol. 32*, 505−513.
33. Morty, R. E., Lonsdale-Eccles, J. D., Mentele, R., Auerswald, E. A., and Coetzer, T. H. (2001) Trypanosome-derived oligopeptidase B is released into the plasma of infected rodents, where it persists and retains full catalytic activity, *Infect. Immun. 69*, 2757−2761.

BI051035K